JGR Biogeosciences

RESEARCH ARTICLE
10.1029/2024JG008189

# Deep-Marine Brine Seeps Stimulate Microbial Nitrogen Cycling: Implications for the Formation of Sediment-Hosted Ore Deposits

**Eva E. Stüeken[1], Annabel Long[1], Nathan Rochelle-Bates[1], and Andreas Teske[2]**

[1]School of Earth & Environmental Sciences, University of St Andrews, Fife, UK, [2]Department of Marine Sciences, University of North Carolina at Chapel Hill, Chapel Hill, NC, USA

**Key Points:**

- Brine seeps in the Gulf of Mexico recycle bioavailable nitrogen from sediments back into the water column
- Nitrogen isotopes suggest that brine seepage stimulates biological activity, including dissimilatory nitrate reduction to ammonium
- Biological productivity stimulated by brine seeps may have contributed to the formation of sedimentary ore deposits

**Supporting Information:**

Supporting Information may be found in the online version of this article.

**Correspondence to:**

E. E. Stüeken,
ees4@st-andrews.ac.uk

**Citation:**

Stüeken, E. E., Long, A., Rochelle-Bates, N., & Teske, A. (2024). Deep-marine brine seeps stimulate microbial nitrogen cycling: Implications for the formation of sediment-hosted ore deposits. *Journal of Geophysical Research: Biogeosciences*, *129*, e2024JG008189. https://doi.org/10.1029/2024JG008189

Received 16 APR 2024
Accepted 24 JUN 2024

**Author Contributions:**

**Conceptualization:** Eva E. Stüeken, Andreas Teske
**Data curation:** Eva E. Stüeken, Annabel Long
**Formal analysis:** Eva E. Stüeken, Annabel Long
**Funding acquisition:** Eva E. Stüeken
**Investigation:** Eva E. Stüeken
**Methodology:** Eva E. Stüeken, Annabel Long, Nathan Rochelle-Bates
**Project administration:** Eva E. Stüeken
**Resources:** Eva E. Stüeken, Andreas Teske
**Supervision:** Eva E. Stüeken
**Validation:** Eva E. Stüeken
**Visualization:** Eva E. Stüeken
**Writing – original draft:** Eva E. Stüeken



**Abstract** Deep-marine brine seeps in the modern ocean are considered analogs for settings that favored the formation of sedimentary-exhalative zinc and lead deposits in deep time. Microbial activity plays an important role in the accumulation of ore minerals, meaning that the extent of mineralization is at least indirectly dependent on nutrient fluxes. Here, we investigated the biogeochemical nitrogen cycle in shallow (15–50 cm) sediment cores from the Orca Basin brine pool and surrounding sites, as well as from an active brine seep area near Dead Crab Lake in the Gulf of Mexico, with the aim of constraining the effect of brine seepage on this bio-essential element. We find high porewater ammonium concentrations in the millimolar range, paired with elevated ratios of organic carbon to nitrogen in sediments, which confirm previous hypotheses that the brine recycles ammonium from sedimentary strata back into the water column. Within Orca Basin, we note tentative evidence of microbial ammonium utilization. At the active seep, ammonium is mixed into the overlying water column and likely undergoes oxidation. Isotopic data from sediments and dissolved ammonium, paired with previously published genomic data, suggest the presence of dissimilatory nitrate reduction to ammonium at the brine-seawater interface. We conclude that brine seeps can stimulate biological nitrogen metabolisms in multiple ways. Our results may help calibrate studies of biogeochemical cycles around brine seeps that are archived in the rock record.

**Plain Language Summary** Brine seeps in the deep ocean are sites where fluids with exceptionally high salinity, up to 10 times that of seawater, seep up through marine sediments and are dispersed into the water column. Such saline fluids can carry high concentrations of metals such as iron, zinc, lead and copper, and therefore brine seeps have been proposed as mechanisms for the formation of ore deposits in the past. An important aspect in this theory is that high microbial activity of primary and secondary producers near the brine seeps creates locally anoxic conditions under which metals are trapped in sulfide minerals. Such biological activity would require input of nutrients, including nitrogen. To shed more light on the biogeochemical nitrogen cycle in brine seeps, we investigated nitrogen isotopes and abundances in samples from the Gulf of Mexico. Here, ammonium concentrations in the millimolar range have previously been documented. Our results support the idea that nitrogen is leached by the brines from deeper sediments and released into the overlying water column. Furthermore, we find evidence for specific microbial metabolisms that are stimulated by mixing between anoxic brine fluids and oxygenated seawater, which may also have occurred in past ore-forming environments.

## 1. Introduction

Anoxic brine pools and saline seeps at the bottom of the ocean with salinities nearly 10 times that of seawater are some of the most extreme environments on the modern Earth (Mapelli et al., 2017; Merlino et al., 2018). They are inhabited by a plethora of microorganisms that capitalize on strong gradients in redox conditions and metabolic substrates. High sulfide concentrations within the brine attest to extensive microbial sulfate reduction, coupled to the oxidation of methane or larger hydrocarbons (Boetius et al., 2005; Lloyd et al., 2010), while sulfide-oxidizing bacteria thrive at the seawater-brine interface on sediment surfaces (Sassen et al., 1993; Teske & Carvalho, 2020). The well-documented, active sulfur cycle makes these environments potential analogs for the formation of sedimentary exhalative (SEDEX) ore deposits in the rock record, where genetic models postulate injection of metal-rich brines into seawater, followed by the generation of anoxic brine pools and trapping of base metals in sulfide minerals (Emsbo, 2009; Sangster, 2018). A famous example is the world-class Pb–Zn SEDEX deposit in

**Writing – review & editing:**
Annabel Long, Nathan Rochelle-Bates, Andreas Teske

the late Paleoproterozoic McArthur Basin (1.6 Ga), where saline brines enriched in metals are thought to have originated from older evaporites deeper within the basin (Large et al., 1998). In this case, a steep geothermal gradient likely facilitated fluid convection and seepage of metal-rich brine into overlying anoxic strata and/or into the water column where sulfide minerals were deposited (Ireland et al., 2004; Williams, 1978).

It has been proposed that the hydrothermal saline seeps of the McArthur Basin also carried with them re-mobilized hydrocarbons (Williford et al., 2011) and ammonium (Stüeken et al., 2021). The latter in particular could have constituted an important source of bioavailable nitrogen to the biosphere, to alleviate N-limitation during the mid-Proterozoic (Anbar & Knoll, 2002). Stimulation of microbial activity by ammonium may have further enhanced anoxia, sulfate reduction and metal accumulation (Magnall et al., 2020). Indeed, modern saline seeps and brine pools are highly enriched in ammonium with concentrations up to 11 mM (Joye et al., 2005, 2010), supporting the idea that such seeps may act as important nutrient point sources. However, our ability to draw comparisons to ancient settings is limited by the lack of detailed investigations of microbial nitrogen cycling in modern environments, in particular with regards to isotopic signatures that can be preserved in the sedimentary record.

To fill this knowledge gap, we measured nitrogen isotopes, along with organic carbon isotopes and ratios of organic carbon to nitrogen in sediment samples from modern saline seeps environments in the Gulf of Mexico. Electrical conductivity (EC), as well as pore fluid concentrations and the isotopic composition of ammonium, were measured to be able to link sedimentary signatures to fluid properties. Our results support the notion that saline seeps act as a recycling mechanism that remobilizes ammonium from sediments (Joye et al., 2005, 2010) and stimulates microbial activity at the brine-seawater interface and possibly at regional scale.

## 2. Study Site

The Gulf of Mexico is partially underlain by salt deposits of Jurassic age that have been deformed into diapirs over nearly 200 million years by tectonism, geothermal heating, and differential loading as the sedimentary overburden has accumulated (Joye et al., 2005; Peel et al., 1995; Pindell & Kennan, 2009). Faults act as fluid conduits along which seawater penetrates into the subsurface and partially dissolves the salt bodies, forming highly saline brines. Geothermal heating creates buoyancy, causing the brines to rise and seep into the basin along faults with temperatures ca. 10–15°C above ambient background (Joye et al., 2005; Roberts & Carney, 1997). Such saline seeps occur in multiple localities around the northwestern Gulf Basin. The most famous locality is the Orca Basin, which is the world's largest submarine brine pool with a brine layer depth of ca. 200 m and a surface area of ca. 400 $km^2$ (Pilcher & Blumstein, 2007; Shokes et al., 1977).

Samples for this study came from three distinct sites (Figure 1, see Table S1 for site coordinates in lat/long). The first set of samples (5 cores), collected by HOV *Alvin* during dive 4650 represents an active brine seep near Dead Crab Lake, a small brine pool (ca. 10 m across) in the Green Canyon area in the Gulf of Mexico (Teske & Joye, 2020), named for the presence of pickled crabs that were trapped in the brine. At the time of sample collection in 2010, the surficial sediments at this location harbored sulfur-oxidizing microbial mats (Stevens et al., 2015; Teske & Carvalho, 2020). The sediment itself is composed of cohesive mostly gray mud. Also, one brine sample from Dead Crab Lake was collected. The second sample set (3 cores, hereafter referred to as slope setting) was collected by HOV *Alvin* (Dive 4650) at the slope of Orca Basin, rising from sediments near the oxycline and halocline that do not contain visible benthos ("Pink Jello" core 4560-5, 2,198 m and "red core" 4560-24, 2,186 m) toward oxic conditions above the halocline and oxycline, evidenced by benthic macrofauna in the form of sponges ("Sponge Garden", core 4650-3, 2,167 m). These characteristics attest to gradually increasing oxic conditions in the water column within this sample set (Nigro et al., 2020). The sediment samples from this site were composed of red to pink mud; sponge fragments were present in the "Sponge Garden" samples. Our third sample set was obtained by multicorer sampling from the consistently hypersaline and anoxic bottom sediments of Orca Basin (Nigro et al., 2020). One core is from the south sub-basin (MUC-6), and one additional sediment sample comes from the north sub-basin (MUC-7). These sediments are composed of poorly consolidated black or dark-gray mud. In addition, we obtained five samples of the brine lake (CTD cast 0502 and Alvin dive 4647). The sediment cores from the three samplings sites were ca. 15–50 cm in length and subdivided into 2–5 cm sections, which were analyzed separately as individual samples. Whenever feasible, sampling sites were recorded with *Alvin's* external camera and automated screen grab system (4dgeo.whoi.edu, Figure 2).

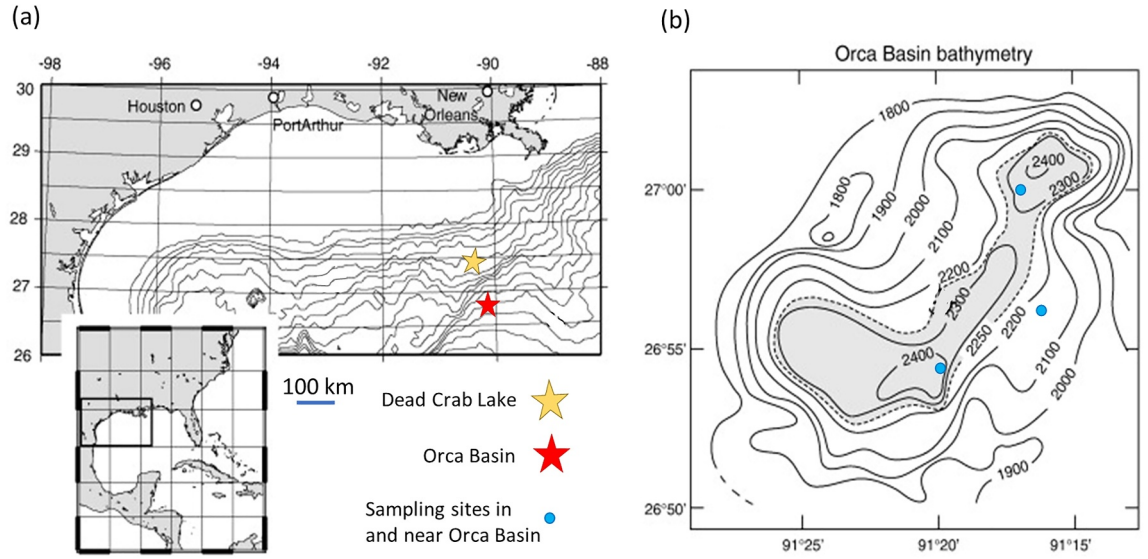


**Figure 1.** Map of the sampling area in the northern Gulf of Mexico. Dead Crab Lake and Orca Basin are located on the Gulf of Mexico slope that is rich in hydrocarbon seeps and brine pools. Modified from Tribovillard et al. (2008).

## 3. Analytical Methods

After collection (Nigro et al., 2020; Teske & Joye, 2020), the samples were stored in the freezer at the University of North Carolina at −80°C. For this project, the frozen samples were shipped to St Andrews in the UK on ice packs. Immediately after arrival, they were fully thawed and then centrifuged at 3,000 rpm for 10 min to separate the sediments from their corresponding pore waters. The pore waters were passed through 0.2 µm PTFE syringe filters (which were washed three times with DI-water), acidified with 100 µl of 1M HCl to limit ammonia ($NH_3$) gas loss, stored in separate Falcon tubes and subsequently kept frozen. The solid sediment residues were placed into a freeze drier for 2–4 days. Once dried, the sediments were pulverized to a fine powder with pestle and mortar and stored in Falcon tubes.

### 3.1. Sediment Decarbonation

Ca. 0.5 g of powdered sediment sample were weighed out into pre-combusted (500°C) glass tubes, mixed with 1 M HCl (10–15 ml) and left overnight at room temperature, with loose caps to allow $CO_2$ degassing. The samples were then centrifuged at 700 rpm for 15 min and the acid was decanted. To ensure complete decarbonation, 1 M HCl was added again for 30 min. If effervescence was observed the samples were left in acid again overnight. After decanting the acid, the samples were washed three times in DI-$H_2O$ (18.2 MΩ cm) and then left to dry at 70°C for 3 days before transfer into pre-combusted scintillation vials.

### 3.2. Organic Carbon and Nitrogen Analyses of Sediments

For analyses of total organic carbon (TOC) and nitrogen content as well as isotopic ratios, ca. 10–15 mg of decarbonated sediment powder were weighed into tin capsules (8 mm height, 5 mm diameter; Elemental Microanalysis) and analyzed by flash-combustion with an elemental analyzer (EA Isolink; Thermo Fisher) coupled via a Conflo IV to a MAT253 isotope ratio mass spectrometer (Thermo Fisher). The EA was equipped with a combustion column packed with $Cr_2O_3$ and silvered cobaltous cobaltic oxide (held at 1,020°C), followed by a reduction column packed with Cu (held at 650°C) and a water trap packed with magnesium perchlorate (held at room temperature). The GC column of the EA was ramped from 40°C to 240°C during each analysis to accelerate elution of $CO_2$. The data were calibrated for TOC and total nitrogen (TN) abundances using a series of USGS-41a standards. The abundance data were initially measured as a mass fraction (expressed in weight percent for carbon and µg/g for nitrogen) and were used to calculate molar C/N ratios by dividing by the molar masses of the two elements: C/N [mol/mol] = (TOC [wt. %]/100/12.01 [g/mol])/(TN [µg/g]/1,000,000/14.01 [g/mol]). Isotopic ratios were calibrated with USGS-41a and USGS-40. The results are expressed in delta notation relative

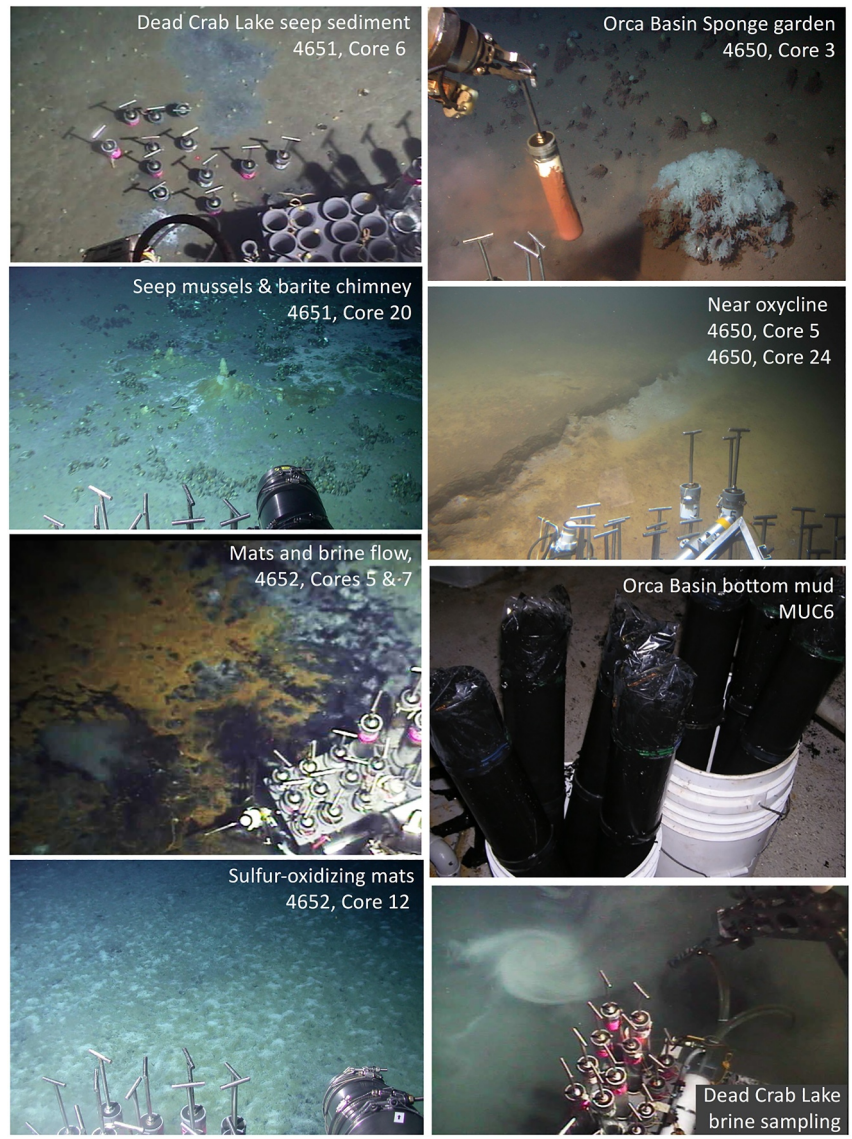


**Figure 2.** Photos showing sampling locations. Images were obtained in situ by Alvin camera and video during Alvin dives 4650 to 4562; the Orca Basin core photos were taken after shipboard retrieval since Alvin cannot dive into the dense brine.

to VPDB for carbon ($\delta^{13}C = [(^{13}C/^{12}C)_{sample}/(^{13}C/^{12}C)_{standard} - 1] \times 1{,}000$) and relative to air for nitrogen ($\delta^{15}N = [(^{15}N/^{14}N)_{sample}/(^{15}N/^{14}N)_{standard} - 1] \times 1{,}000$). USGS-62 and SDo-1 were analyzed for quality control, and the measured results (USGS-62: $\delta^{13}C = -14.79 \pm 0.07‰$ (1SD), $\delta^{15}N = 20.38 \pm 0.17‰$ (1SD), $n = 30$; SDo-1: $\delta^{13}C = -30.25 \pm 0.04‰$ (1SD), $\delta^{15}N = -0.53 \pm 0.27‰$ (1SD), $n = 15$) are in good agreement with expected values (USGS-62: $\delta^{13}C = -14.79 \pm 0.04‰$, $\delta^{15}N = 20.17 \pm 0.06‰$; SDo-1: $\delta^{13}C = -30.0 \pm 0.1‰$, $\delta^{15}N = -0.8 \pm 0.3‰$) (Dennen et al., 2006; Schimmelmann et al., 2016).

### 3.3. Ammonium Quantification in Pore Waters

A colorimetric method was used to determine the concentration of dissolved ammonium ($NH_4^+$) in pore waters (Cleaves et al., 2008). Analysis of the samples were carried out using the Thermo Fisher Scientific Evolution Series 200 UV-Visible Spectrophotometer at a wavelength of 640 nm. All reagents were prepared using pre-combusted glassware (500°C) and DI-$H_2O$ (18.2 MΩ cm), including the sodium citrate buffer (7.6 g of trisodium citrate and 0.4 g of sodium hydroxide in 500 ml of DI-water), phenol alcohol (1 ml liquefied phenol with 90 ml of 100% ethanol, brought up to 100 ml using DI-water) and aqueous sodium nitroprusside (0.15 g of sodium

nitroprusside dissolved in 200 ml of DI-water). These were stored in the fridge for several weeks. An oxidizing solution was prepared daily from 10 ml of the sodium citrate buffer and 0.1 ml of aqueous sodium hypochlorite (10%–15% available chlorine). Calibration standards ranging from 0.5 to 100 µM were prepared using a stock solution of 1 mM $NH_4Cl$. Samples were diluted with DI-$H_2O$ to fall within this range. This range was chosen because here the measured adsorption by the coloring complex is linearly correlated with ammonium concentration. To each 1 ml of standard or sample, 0.5 ml of phenol alcohol, 0.5 ml of aqueous sodium nitroprusside and 1 ml of oxidizing solution were added within 15 ml Falcon tubes. The mixture was left to sit at room temperature for 60–80 min and then transferred to cuvettes for analysis. Average reproducibility was 1.6% with a maximum of 8%.

### 3.4. Ammonium Microdiffusion Method for Dissolved $NH_4^+$ Isotopic Analysis

In a subset of samples from the active seep near Dead Crab Lake and from the Orca Basin brine pool, we analyzed the isotopic composition of the dissolved ammonium by microdiffusion (Zhang et al., 2016). First, glass fiber filter disks with a diameter of 5 mm were cut from a 10 mm diameter Whatman GF/D filter using a hole punch (cleaned with methanol). The disks were then placed on a $5 \times 1$ $cm^2$ strip of Teflon tape, and 10 µl of 2.5 M $H_2SO_4$ were pipetted onto the disk. Using tweezers, the Teflon tape was folded and sealed around the disk with the odd end of a pipette tip. Excess Teflon tape around the edges was cut off with scissors.

Solutions containing dissolved ammonium were diluted with DI-water to ammonium concentrations of 100 µM in a 10 ml volume. The dilutions were done in 20 ml glass vials. To maintain a balanced osmotic gradient across the Teflon tape and prevent rupture of the acid traps, 0.7455 g of KCl (Sigma-Aldrich, Cat No. 7447-40-7) were added to each vial to achieve a 1 M concentration. Then one acid trap was added to each vial along with a magnetic stir bar (approximately 5 mm in length). Ca. 100 mg MgO (ThermoScientific, Cat No. 205155000) were added, and the vials were capped immediately with a septum and crimp cap. The mixture was then shaken to help homogenize the MgO in the solution. The vials were placed on magnetic stir plates in sand baths at 70°C for 4 days. After incubation, the acid traps were removed from the vials, dipped in 1 M HCl, and briefly rinsed with DI-$H_2O$. The Teflon tape was pulled open, and the filters were placed into a freeze-drier for 2 days. Blanks with no ammonium addition were prepared in the same way. Further, a "freeze-drier blank" acid trap was placed into the freeze drier to ensure that no absorption of ammonia gas occurred during the drying process. Three international ammonium sulfate standards were used for calibrating this method (IAEA-N-1, IAEA-N-2, and USGS-25). For each one, we prepared a 15 ml stock solution of 1 mM ammonium and doped it with 10 µl of 1 M HCl to prevent loss of ammonia gas during storage. For all samples and standards, the dried filters were transferred into tin capsules and analyzed by the same EA-IRMS setup as the sediment samples. IAEA-N2 and USGS-25 were used to calibrate the isotopic ratios and IAEA-N1 was used for quality control. The measured results ($\delta^{15}N = 0.22 \pm 0.34‰$, $n = 8$) are in good agreement with the expected value ($\delta^{15}N = 0.43 \pm 0.14‰$) (Gonzalez & Choquette, 2023).

### 3.5. Electrical Conductivity

For each sample site, one core was selected to measure the EC of the pore fluids (*i.e.*, using the same pore fluids as for ammonium measurements above). These measurements were done with a Hanna EC probe, connected to a Hanna benchtop multi-meter. Prior to analyses, the probe was calibrated with a series of conductivity standards from Hanna, ranging from 84 µS/cm to 80'000 µS/cm. A 30 ml volume of each sample was prepared with a 100-times dilution in plastic 50 ml centrifuge tubes. The conductivity reading was taken once the reading had stabilized.

## 4. Results

A digital version of all data is available through the National Geoscience Data Center of the British Geological Survey (Stüeken et al., 2024). The EC profiles from representative sediment cores at the three sampling sites (Table S1, Figure 3) show consistently high values (524–550 mS/cm) within the Orca Basin brine pool sediments and consistently low values in the slope sediments from and above the oxycline (79–83 mS/cm). The active seep near Dead Crab Lake shows a gradient from 182 mS/cm at the top to 419 mS/cm at the bottom of the core. These results are consistent with visual observations of dense, reducing brine filling the coring holes during sampling. The contrasting conductivity profiles confirm the distinct characters of the three sampling sites.

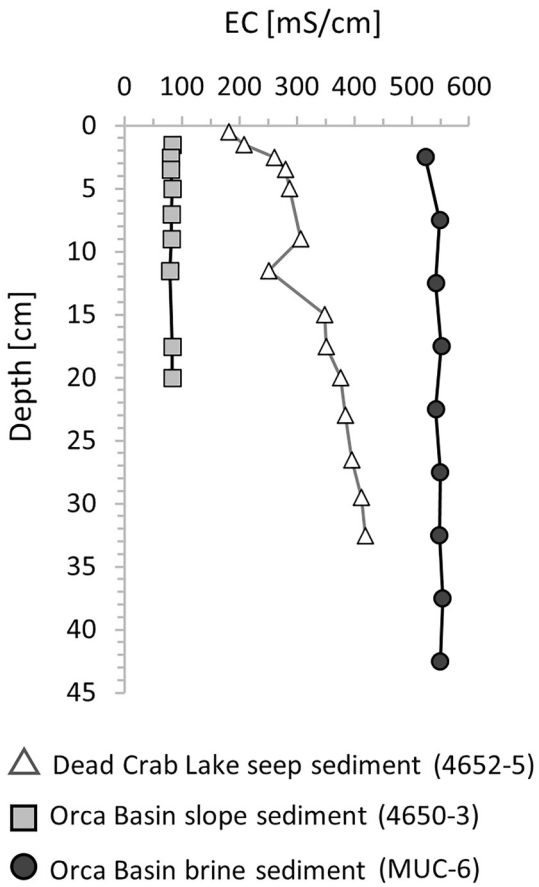


**Figure 3.** Electrical conductivity profiles in sedimentary pore fluids. Representative cores from the three types of settings were chosen.

The $\delta^{15}N$ values of the sediment samples (Table S1) from the Orca Basin slope (mean = 3.0 ± 0.7‰, 1SD, Figure 4e) as well as from the Orca Basin bottom sediment (2.7 ± 0.2‰) (Figure 4i) are similar to the composition of dissolved nitrate in seawater in the Gulf of Mexico (2.5‰, Meckler et al., 2011). Only slope core 4650-3 above the oxycline ("Sponge Garden") is overall slightly enriched in $^{15}N$ to ca. 3.5‰ (removing this core from the mean reduces the average composition of the slope sediments to 2.7 ± 0.5‰). Organic carbon isotopes ($\delta^{13}C$) are similarly stable and show only a subtle difference between the Orca Basin slope (−22.7 ± 0.7‰, Figure 4g) and the brine pool sediment (−21.8 ± 0.1‰, Figure 4k). Molar ratios of organic carbon to total nitrogen (hereafter C/N) for the two sites are all between 10 and 13 (brine pool: 10.2 ± 0.1, Figure 4l; slope site: 11.0 ± 0.7, Figure 4h).

At the active seep near Dead Crab Lake, the sediments display $\delta^{15}N$ values only slightly above seawater nitrate in the bottom of all cores (Figure 4a), but in the top 5–10 cm, all cores show a shift toward lighter values where the minimum value always occurs in the top-most sample and ranges from −1.5‰ to +0.3‰ across the five cores. Organic $\delta^{13}C$ decreases in parallel with $\delta^{15}N$ (Figure 4c). At the bottom, all cores show $\delta^{13}C$ values around −26‰ to −27‰, while the core tops decrease to values around −30‰ or less. The lowest value of −41.4‰ is found 2–3 cm below the surface in core 4652-5. Molar C/N ratios are mostly above 10 at depth in all cores, but the core tops show a consistent decrease in C/N with a minimum of 7 found at the top of core 4652-5 (Figure 4d). In consequence, $\delta^{15}N$ and C/N are strongly correlated across the active seep site ($R^2 = 0.65$, $p < 10^{-12}$).

When the total N (TN) content of the decarbonated residues is plotted versus TOC (Figure 5), we find that the samples from the Orca Basin brine pool and the slope site fall along a continuum, attributable to their consistent C/N ratios. TN and TOC across all samples from both sites are strongly correlated ($R^2 = 1.0$, $p < 10^{-50}$) with a TN intercept of −0.01 wt. % (Figure 5). In the sediments from the active seep near Dead Crab Lake, we find that the core tops with C/N < 10 fall along a steeper slope compared to the core bottoms with C/N > 10. In both cases, the two parameters are strongly correlated ($R^2 = 0.99$ and 0.83, respectively, $p < 10^{-6}$). The TN intercept is +0.02 wt. % in the subsurface and −0.09 wt. % in the core tops.

Dissolved ammonium in pore waters (Table S1) is mostly below 0.3 mM in the sediments from the Orca Basin slope; only few outliers exceed this threshold (Figure 4f). The mean is 0.16 + 0.28/−0.16 mM (median 0.09 mM). Brine samples from within 100 m of the surface of the Orca Basin Brine pool are slightly enriched in ammonium to up to 0.5 mM in the northern sub-basin (Table S2). Within the Orca Basin brine pool sediments, dissolved ammonium concentrations display a mean of 1.38 ± 0.14 mM (Figure 4j). For the Orca Basin brine pool and porewater samples, we were able to obtain $\delta^{15}N$ isotopic measurements of the dissolved ammonium and found most of the sedimentary samples to cluster around a mean of 4.5 ± 0.3‰, systematically offset from the solid sedimentary values by 1.8 ± 0.3‰ on average (Figure 4i). The top-most pore water sample is an outlier with a $\delta^{15}N$ value of 8.6 ± 0.5‰ for dissolved ammonium, confirmed with a replicate measurement. This value is offset from the corresponding sediment by 5.7 ± 0.5‰. The brine from the overlying basin (5.2 ± 0.1‰ and 4.5 ± 0.2‰ at the two sites) is only slightly enriched in composition to the lower sedimentary pore waters.

In the sediments from the active seep area near Dead Crab Lake, dissolved ammonium concentrations broadly decrease up-section in all cores (Figure 4b). The gradient, defined here as the ratio of the maximum ammonium concentration at the base of each core to the minimum concentration at the top, ranges from 2.1 to 4.6. The highest concentrations with up to 8.5 mM were measured in core 4652-5 with a gradient of 3.3. For comparison, the gradient in EC in the same pore fluids is 2.3 (Figure 3). From this core, we also obtained isotopic data for the dissolved ammonium (Figure 4a). In the lower part of the core, the dissolved ammonium is offset in $\delta^{15}N$ from the sediments by 0.9 ± 0.2‰ on average, but the offset increases to up to 4.6 ± 0.6‰ at the top. In other words, the dissolved ammonium shows a more subtle decrease in $\delta^{15}N$ at the top of the core by only about 1‰ compared to a

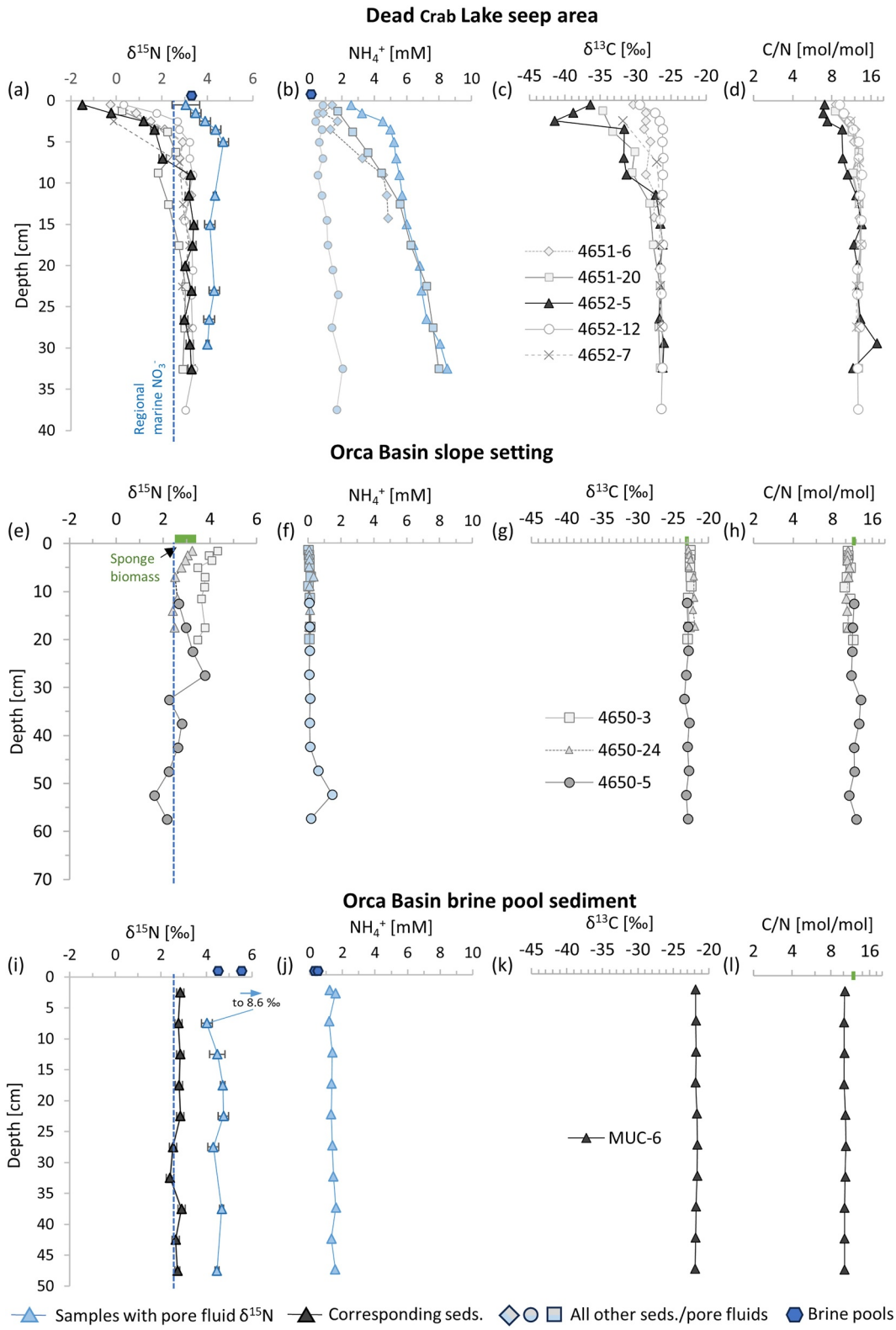


**Figure 4.**

decrease by ca. 4.5‰ seen in the sediment samples over the same interval. The brine sample from Dead Crab Lake is similar to the upper pore waters, showing a value of 3.3 ± 0.1‰.

## 5. Discussion

### 5.1. Sedimentary Archive of Marine Nitrate in Orca Basin

The Gulf of Mexico is generally described as oligotrophic with high rates of biological $N_2$ fixation occurring in surface waters, making it a net source of fixed nitrogen to the global ocean (Gruber & Sarmiento, 1997). Biological $N_2$ fixation generates biomass with an isotopic composition around −1‰ (Carpenter et al., 1997; Minagawa & Wada, 1986). As this biomass is remineralized during sinking through the oxic water column, it is rapidly oxidized to nitrate, which adopts the same isotopic composition (Marconi et al., 2019). Globally, the marine nitrate pool is slightly enriched in $^{15}N$ due to partial nitrate reduction (denitrification) to $N_2$ in oxygen-minimum zones, giving it an average $\delta^{15}N$ value of ca. 5‰ (Brandes & Devol, 2002; Sigman et al., 2000). Mixing between nitrate from the open Atlantic and nitrate regenerated from biomass locally thus explain the $\delta^{15}N$ value of ca. 2.5‰ for nitrate dissolved in water column in the Gulf of Mexico (Knapp et al., 2005; Meckler et al., 2011).

This value of 2.5‰ closely matches the composition of many of the sediment samples from the Orca Basin brine pool and the surrounding inactive areas (Figures 4e and 4i). This match is consistent with the notion that biomass buried on the seafloor represents an isotopic archive of the nitrate that is dissolved in the overlying water column (Altabet & Francois, 1994; Tesdal et al., 2013). Nitrate is the major form of bioavailable nitrogen in the modern ocean, and nitrate-assimilating organisms adopt its isotopic composition, especially where nitrate is a limiting nutrient, leading to quantitative uptake into biomass without net isotopic fractionation. In fact, this property has previously been exploited by Meckler et al. (2011), who investigated nitrogen isotopes in one core from Orca Basin with a depth range from 38 to 898 cm (*i.e.*, more extensive but at lower resolution than in this study) and used the data to draw inferences about the evolution of $\delta^{15}N$ in the marine nitrate pool over the past 25,000 years. Their results from the upper meter (<3,000 years) are in good agreement with our data. The conclusion that these sediments archive the isotopic composition of marine nitrate in the form of nitrate-assimilating biomass is further supported by the strong correlation between TN and TOC with minimal TN intercept (gray and black data points in Figure 5), which indicates that most of the nitrogen in our sediment samples from the Orca Basin and surroundings is likely organic-bound or directly derived from biomass.

It has long been known that dissolved ammonium is highly enriched in the Orca Basin brine pool (Joye et al., 2005; Nigro et al., 2020; Van Cappellen et al., 1998; Wankel et al., 2010) compared to average seawater (<0.1 μM, Cowen et al., 1998). This is also seen in our own brine data, which show ammonium concentrations of ca. 0.5 mM within the Orca Basin and over 1 mM in the underlying sedimentary pore waters (Table S2). Joye et al. (2005) attributed these high concentrations to three possible sources, including (a) decomposition of sinking organic matter, (b) desorption of ammonium from sinking inorganic particles, and (c) desorption of ammonium from deeper sedimentary strata as the brine rises to the seafloor. Ammonium can adsorb to and become incorporated into clay minerals in substitution for potassium (relevant to process *b* and *c*), as both ions have the same charge and similar radii (Abdulgawad et al., 2009; Yu et al., 2023). This substitution typically occurs during diagenesis, when ammonium is released from organic matter and appears in close contact with the sedimentary clay matrix (relevant to *c*) (Müller, 1977; Schroeder & McLain, 1998). This adsorbed ammonium can be displaced by other cations, meaning that adsorption decreases with increasing salinity (Rysgaard et al., 1999; Yu et al., 2023). Therefore, the high ionic strength of the brine that rises up through the sedimentary package may desorb ammonium that was previously stored in clay particles, possibly deeper down in the sediment column (see

**Figure 4.** Stratigraphic columns of sedimentary (gray and black) and pore water (blue) data. (a)–(d) = Dead Crab Lake area; (e)–(h) = Orca Basin slope setting; (i)–(l) = Orca Basin interior. Sediment data were measured after removal of pore waters and after washing with HCl and DI-water. Vertical dashed blue line in panels (a), (e), and (i) marks the composition of dissolved seawater nitrate in the Gulf of Mexico (Meckler et al., 2011). The sponge biomass shown for the Orca Basin Slope setting represents material collected from the surface near the coring site. Error bars for the $\delta^{15}N$ data from pore fluids (blue triangles) are ±1 σ. Sedimentary data from the same samples as used for pore fluid isotopic data are labeled corresponding seds (black triangles). Where replicates were not measured, the average standard deviation from all other samples is plotted. Blue hexagons show the compositions of the brine pool sample. The *y*-axis (sediment depth) does not apply to these samples. Note that the ammonium concentration of the brine pools like likely lower than that of the pore waters because the brine samples were taken from near the brine-seawater interface and are therefore more diluted by seawater.

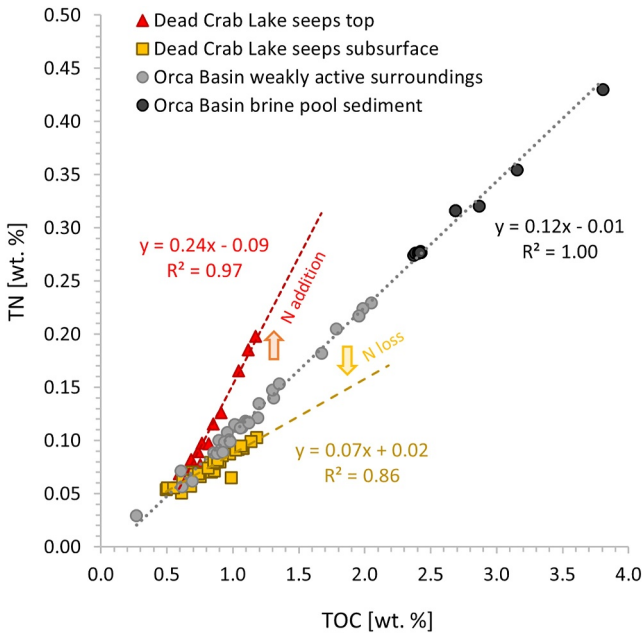


**Figure 5.** Total nitrogen versus total organic carbon in solids. The shallow slope of the regression line through the subsurface samples from the seep near Dead Crab Lake (C/N > 10, yellow) suggests N loss relative to the core tops (C/N < 10, red). Dead Crab Lake core tops are enriched in N compared to the Orca Basin sediments.

also Yamanaka et al., 2024). Hence, while all three processes likely contribute to ammonium input, process *c* is perhaps the most significant (see also Section 5.2).

Meckler et al. (2011) report bulk sedimentary $\delta^{15}N$ values up to 4‰ at 3 m depth, and so it is conceivable that the isotopic offset that we observed between the dissolved ammonium and the bulk sediments in our Orca Basin brine pool samples (core MUC_6, Figure 4i) represents upwards seepage of ammonium that was derived from sediments with a different isotopic composition. Alternatively, it is possible that the ammonium was derived from biomass or clays locally but with a small isotopic fractionation. For example, preferential degradation of isotopically enriched proteins relative to other biomolecules (Macko et al., 1987) may have generated an isotopically enriched ammonium pool in pore waters. Alternatively, the isotopic offset between dissolved ammonium and solid sediments may represent equilibrium fractionation between dissolved and adsorbed ammonium (Li et al., 2021).

Intriguingly, the ammonium $\delta^{15}N$ value of the top-most fluid sample from the Orca Basin brine core (MUC-6) is offset by 5.7‰ from its corresponding sediment sample (Figure 4i). Since we have only one data point, this observation is difficult to interpret. But if real, we speculate that it may represent a local biological effect, such as partial ammonium assimilation or nitrification/anammox. Ammonium assimilation imparts a fractionation of 14–27‰, rendering the residual ammonium isotopically heavy (Hoch et al., 1992; Waser et al., 1998). Extremophiles residing in the brine pool may potentially perform this metabolism. While we did not find the corresponding isotopically light biomass of such ammonium-assimilating extremophiles in the Orca Basin sediments, it is possible that this component is swamped by the overwhelming influx of organic particles from above.

We note that core 4650-3 from the slope immediately surrounding the Orca Basin brine pool shows $\delta^{15}N$ values that are ca. 1–2‰ higher than the composition of marine nitrate, making this core distinct from all other cores from the Orca Basin. This core was taken above the halocline and oxycline on the slope of the brine pool (Nigro et al., 2020) where aerobic plankton and benthos thrive. If so, then locally quantitative assimilation of isotopically enriched ammonium into biomass may explain the slightly elevated sedimentary $\delta^{15}N$ values. Interesting to note is that sponges, which occur at this site, are known to consume microbial biomass (Hanz et al., 2022), and hence N-fueled microbial mats may drive sponge growth at this location.

In conclusion, the data from the Orca Basin brine pool and its surroundings support the notion that the isotopic composition of marine nitrate is well preserved in briny sedimentary organic matter. Furthermore, we find tentative evidence for biological utilization of the brine-sourced ammonium at the sediment-brine interface and in the surrounding slope setting that displays an unusually high activity of sponges.

### 5.2. Nitrogen Redox Cycling in Active Seeps Near Dead Crab Lake

A striking feature of the active seep sediments near Dead Crab Lake compared to the sediments from within and around Orca Basin is the drop in $\delta^{15}N$ and C/N in the top few centimeters of all cores while both parameters are enriched at depth. The relatively elevated C/N ratios in the subsurface of these cores likely reflects leaching of ammonium by the saline fluids as they seep upwards. As noted above, ammonium is released from degrading biomass, and it tends to adsorb less strongly to clay minerals at high salinity. Previous studies have therefore speculated that seepage of saline fluids through the sediment package is an effective mechanism of exporting ammonium (Joye et al., 2005), and our data provide direct evidence for this process (i.e., process *c* listed above). The $\delta^{15}N$ enrichment in these subsurface sediments compared to background marine nitrate (Figure 4a) may thus represent a kinetic effect whereby isotopically light ammonium is exported preferentially. We note that this kinetic effect would counteract the equilibrium isotope effect discussed above in the context of core MUC-6 in the Orca brine poo. In parallel, isotopically heavy ammonium of deep subsurface origin (Yamanaka et al., 2024) could contribute toward shifting the $\delta^{15}N_{NH4+}$ values for this core toward $\delta^{15}N$ enrichment (Figure 4a).

The decrease in C/N in the core tops indicates enrichment in N compared to normal marine sediments, as represented by the sediment cores surrounding Orca Basin (Figure 5). Previous studies identified microbial mats at the sampling site near Dead Crab Lake, including abundant sulfide oxidizers such as *Beggiatoa* that are known to actively accumulate nitrate in their cells (Salman-Carvalho et al., 2016; Stevens et al., 2015). It is likely that our sample preparation protocol washed out most nitrate from the samples because (a) nitrate is highly soluble in water, and (b) cells containing nitrate may have been ruptured during centrifugation and freeze-drying; however, the N-enrichment may be a relic of biological nitrate uptake, if followed by conversion into organic-bound N.

The isotopic data provide additional insights into this process. In the core tops, $\delta^{15}N$ drops to values as low as −1.5‰ (Figure 4a). Such values fall within the range of biological $N_2$ fixation (Carpenter et al., 1997; Minagawa & Wada, 1986; Zerkle et al., 2008; Zhang et al., 2014). Usually, this metabolism occurs in settings characterized by N-limitation, but is has been described from benthic ammonium-rich environments where it is thought to serve as an electron sink (Knapp, 2012). Genomic evidence of the nitrogenase enzyme, which catalyzes $N_2$ fixation, has been described from an ammonium-rich brine seep in the Mediterranean where it may be involved in the production of osmo-protectants (Merlino et al., 2018; Pachiadaki et al., 2014). We cannot completely rule out this possibility as an explanation for the observed drop in $\delta^{15}N$ in our near-surface samples; however, it is not obvious why this process would be occurring preferentially at the sediment-water interface, which is also the interface between anoxic brine and oxic seawater (Teske & Joye, 2020), and not within any of the Orca Basin slope sediments, which still contain dissolved ammonium above marine background.

Another possible biological process is partial ammonium assimilation by organisms that are feeding on the ammonium brought up by the brine seepage. This interpretation would be consistent with the drop in ammonium concentrations in the pore waters. As noted above, ammonium assimilation imparts a fractionation of 14–27‰ and may thus explain the production of isotopically light biomass (Hoch et al., 1992; Waser et al., 1998). However, this metabolism would generate isotopically enriched ammonium, while our measurements of $\delta^{15}N$ in pore waters show a decrease at the top, concurrent with the drop in sedimentary $\delta^{15}N$ (Figure 4a). Likewise, partial ammonium oxidation (aerobically or anaerobically) is expected to generate isotopically heavy ammonium (Brunner et al., 2013; Casciotti et al., 2003), inconsistent with the fluid data.

Instead, the most parsimonious explanation for isotopically light ammonium is DNRA. This metabolism imparts an isotopic fractionation of ca. 30‰, where the resulting ammonium is isotopically depleted (McCready et al., 1983). DNRA may be coupled to sulfide oxidation (Schutte et al., 2018), for which there is evidence in the Dead Crab Lake microbial mats (Stevens et al., 2015; Teske & Carvalho, 2020; Teske & Joye, 2020). The endmember brines are enriched in dissolved sulfide by a few mM (Salman-Carvalho et al., 2016). If nitrate-assimilating sulfide oxidizers reduce over 90% of their accumulated nitrate and store some of the resulting ammonium in their biomass, this could explain the observations (Figure 6). If some of the resulting isotopically light ammonium is released and mixed with ambient ammonium from the brine, this process could explain our collective data set, including the drop in sedimentary C/N and $\delta^{15}N$ as well as fluid $\delta^{15}N$. A smaller degree of nitrate reduction would also be possible if mixing between N-sources is taken into account. For example, 80% nitrate reduction by DNRA may generate biomass and ammonium with a $\delta^{15}N$ composition around −10‰, which may be pushed up to the measured values if mixed with background biomass sinking down from the sea surface (2.5‰, see Orca Basin, Figure 4i) and with ammonium from the brine deeper in the same core (4.5‰, Figure 4a), respectively. In either case, the residual isotopically enriched nitrate (Figure 6) would be small in abundance and become diluted by the larger marine nitrate reservoir. The DNRA model requires that some of the resulting ammonium is retained within biomass, which is effectively equivalent to assimilatory nitrate reduction. Previous studies have tried to disentangle the relative proportions of the two different pathways (*i.e.*, nitrate assimilation and nitrate reduction to excreted ammonium) yielding estimates ranging from a few percent to over 90% for the latter (reviewed by Rütting et al., 2011). This measurement is notoriously difficult due to multiple competing metabolisms occurring at redox interfaces. We cannot easily resolve this problem here, but the observation that both processes can occur in tandem supports our overall conclusion.

One aspect that remains unexplained by this scenario is the drop in ammonium concentrations up-section in all cores (Figure 4b), although DNRA generates additional ammonium. This drop may in part be explained by mixing between ammonium-rich brine and ammonium-poor seawater (Van Cappellen et al., 1998). However, the drop in ammonium in core 4652-5 is larger than the drop in EC (factor of 3.3 vs. 2.3), pointing toward an additional ammonium sink. We propose that this additional sink is (aerobic or anaerobic) ammonium oxidation

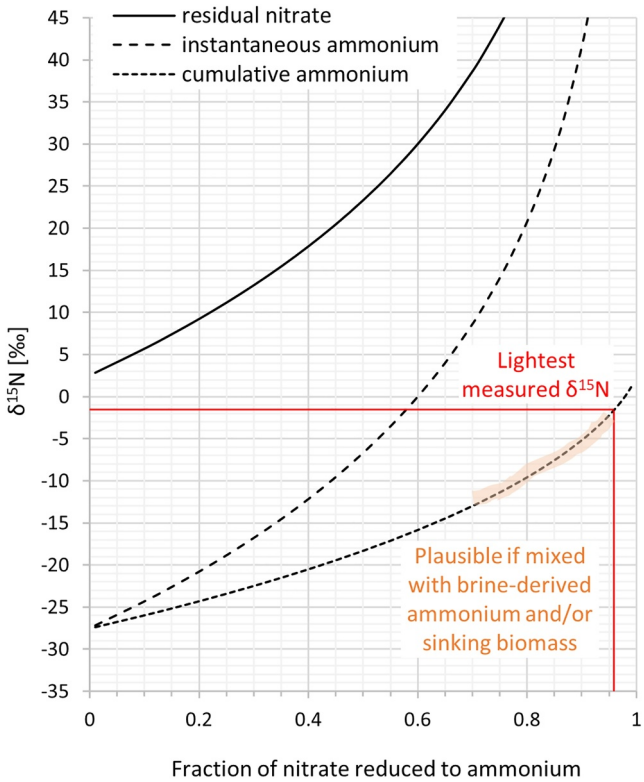


**Figure 6.** Rayleigh model of dissimilatory nitrate reduction to ammonium. The model is based on a fractionation of 30‰ and a starting composition of 2.5‰ for the initial nitrate (Meckler et al., 2011). With these parameters, over 90% nitrate reduction are required to explain the light $\delta^{15}N$ value measured within biomass in the Dead Crab Lake seep sediments (Figure 4). Lower degrees of reduction may be possible, if the resulting isotopically light ammonium is mixed with isotopically heavy ammonium coming up from the brine or, in the case of biomass, if it is mixed with sinking organic matter. Dissolved ammonium may further be pushed to heavier values by partial oxidation or assimilation (see text).

above the sediment-water interface, given the strong redox gradient between the brine and the overlying water column (Teske & Joye, 2020). The isotopic effect of this process (1–25‰ for net oxidation of ammonium to nitrate, Casciotti, 2009), which should generate ammonium enriched in $\delta^{15}N$, is perhaps camouflaged by the isotopic signal of DNRA (30‰, McCready et al., 1983) that operates in the opposite direction. Genomic evidence of ammonium-oxidizing Archaea (AOA) has been retrieved from brine seeps in the Red Sea and in the Mediterranean (Merlino et al., 2018), and ammonia-oxidizing archaea are abundantly associated with sulfur-oxidizing microbial mats and surficial sediments in Guaymas Basin (Engelen et al., 2021; Winkel et al., 2014). 16S rRNA gene sequences of AOA have also been obtained from briny seep sediments in the Gulf of Mexico (Lloyd et al., 2006). Further evidence for oxidative processes at the sediment-water interface at our sampling site near Dead Crab Lake comes from the drop in $\delta^{13}C$ at the very top of the cores, which may be indicative of methanotrophy taking advantage of the interface between methane-rich brine and oxic seawater (Grey, 2016). The presence of sulfate-reducing and methanotrophic consortia in brine seeps in the Gulf of Mexico has also been demonstrated on the basis of phylogeny and organic geochemistry (Boetius et al., 2005). Methane and other hydrocarbons are mostly brought up along with the brine, mobilized from deeply buried biomass or by the destabilization of gas hydrates.

In conclusion, our data suggest that in the active seep near Dead Crab Lake the influx of anoxic sulfide-rich brine stimulates DNRA at the brine-seawater interface (Figure 7), despite the presence of elevated ammonium concentrations in the brine fluid. However, we also see tentative evidence of ammonium consumption, possibly via aerobic or anaerobic oxidation. In any case, the concurrent drop in ammonium concentration and EC shows that ammonium is mixed into the overlying water column. Here, it likely undergoes complete oxidation and mixing with the marine nitrate pool. The brine seeps near Dead Crab Lake thus constitute a source of recycled fixed nitrogen into marine environments.

### 5.3. Broader Implications

Brine seeps enriched in base metals have been implicated in the formation of sediment-hosted ore deposits (Emsbo, 2009; Large et al., 1998; Sangster, 2018). In these settings, microbial activity at the brine-seawater interface may play a role in precipitating sulfide minerals of economic value (Lyons et al., 2006; Magnall et al., 2020; Southam & Saunders, 2005). Similar to the brines in the Gulf of Mexico, ancient ore-forming fluids may have been enriched in ammonium that was leached from older sedimentary strata (Stüeken et al., 2021). The results from this study provide additional evidence of ammonium leaching by rising brine (Figure 5), confirming previous hypotheses (Joye et al., 2005). Of course, we emphasize that the system studied here is merely an analog and more work will be needed to verify that similar processes occurred in ancient settings. Nevertheless, our results suggest that in the context of ore-formation, where it is critical to maintain anoxic conditions via high microbial productivity, the provision of bioavailable ammonium by the metal-rich brines may be a key parameter. Previous work on a large economic SEDEX deposit in the McArthur Basin in Australia identified a 4‰ gradient in $\delta^{15}N$ with lower values (ca. 3.5‰) near the ore zone and higher values in more distal sediments (ca. 7.5‰) (Stüeken et al., 2021), which was at the time interpreted as hydrothermal nitrogen input with a light isotopic composition. The data from this work indicate that such light values near the locality of brine injection may also result from secondary metabolisms, stimulated by brine-sourced metabolites.

The presence of brine seeps has further been invoked for the middle Cambrian Burgess Shale environment that hosts some of the most famous animal fossils from the Cambrian explosion (Johnston et al., 2009; Powell et al., 2006). Dolomite and meter-scale chlinochlore laminates enriched in magnesium have been identified at several localities within the Burgess Shale Formation, which was deposited in a basinal environment. These

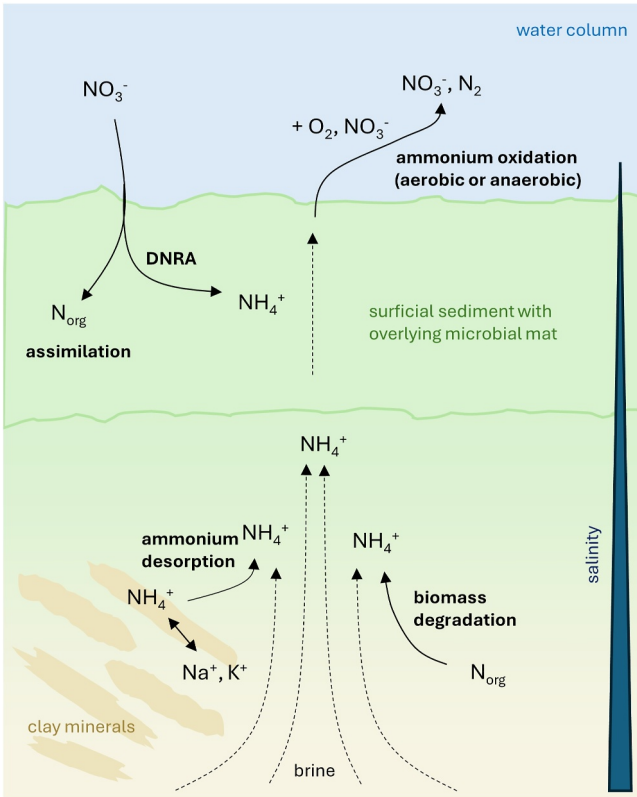


**Figure 7.** Schematic of proposed nitrogen cycling at brine seeps such as Dead Crab Lake. Solid arrows = chemical transformation; dashed arrows = transport.

enrichments are believed to represent anoxic Mg-rich brine pools that formed at the base of a carbonate platform escarpment. Although these brine pools have not been identified at every fossiliferous Burgess Shale outcrop locality, fossil distributions suggest that the pools concentrated megafauna around them as a result of increased microbial productivity (Johnston et al., 2009), possibly akin to the high activity of sponges seen in the slope setting in our study, abundant sediment-feeding sea urchins and holothurians around Alaminos Canyon brine pool, or crabs and mussels around (and sometimes within) Dead Crab Lake (Teske & Joye, 2020). We speculate that remobilized ammonium may have played a key role in driving this locally enhanced productivity. Burgess Shale Type preservation has been critical for our understanding of early Phanerozoic ecology (Gaines, 2014), preserving soft-bodied animals in exquisite detail (e.g., Parry & Caron, 2019), in addition to shelly fauna. The environmental factors that influence this type of preservation are key to recognizing possible taphonomic biases in the rock record. The microbial and redox processes highlighted in this study provide an important reference point for interpreting taphonomic processes that may have operated around Cambrian brine seeps and influenced Burgess Shale-type preservation locally.

Lastly, our work highlights the difficulty of identifying DNRA in the sedimentary record. The isotopic trends at the brine-seawater interface at the active seep near Dead Crab Lake in the Gulf of Mexico can be linked to DNRA (Figure 4a), because we have the luxury of paired isotopic records of sedimentary biomass and dissolved ammonium, as well as support from previously published microbial observations and genomic data (Schutte et al., 2018; Stevens et al., 2015; Teske & Carvalho, 2020; Teske & Joye, 2020). In deep time, only the sedimentary record is available, and it would be difficult to reconstruct the presence of DNRA from this record alone, because the isotopic signature overlaps with that of other metabolisms. Our results therefore suggest that DNRA may be more prevalent at anoxic-oxic interfaces than previously thought. In fact, DNRA is a more efficient electron sink (eight electrons per nitrate molecule) compared to denitrification (five electrons per nitrate molecule), which may constitute an advantage when electron acceptors are limited (Teske, 2010). Tracking DNRA is further important, because unlike canonical denitrification or anammox, which both generate $N_2$ gas, DNRA retains bioavailable nitrogen in the system, making it advantageous for N-starved ecosystems. Widespread DNRA in the Precambrian ocean may thus help resolve a major nutrient limitation (Anbar & Knoll, 2002).

## 6. Conclusions

Modern brine seeps are important analogs for the formation of SEDEX ore deposits that host some of the major economic reserves of base metals (Large et al., 2005). They may also be important for understanding the distribution and preservation of animal fossils in the world-famous Burgess Shale (Gaines et al., 2012; Johnston et al., 2009). Both processes, that is, ore deposition and fossil preservation, are influenced by microbial activity and therefore require a thorough understanding of nutrient sources. Modern seep environments can thus serve as calibration points for nutrient fluxes and geochemical signatures that may be archived in the rock record.

Our data from the modern Gulf of Mexico, including the Orca Basin brine pool, its immediate surroundings, and an active seep are near Dead Crab Lake, support the notion that brine seeps carry with them bioavailable ammonium, mobilized from deeper sedimentary strata (Joye et al., 2005). While the modern ocean is relatively enriched in nitrate (ca. 30 μM, Gruber & Galloway, 2008), such a recycled ammonium flux from brine seeps may have constituted a major point source of a bio-essential nutrient in the Precambrian, when the ocean was likely N-depleted compared to today (Anbar & Knoll, 2002; Koehler et al., 2017; Stüeken et al., 2021), and it may have facilitated the preservation of animal fossils underneath microbial mats in the Cambrian and beyond.

In this modern setting, where the brine-seawater interface is at the same time an interface between anoxic and oxic fluids (Teske & Joye, 2020), the brine seepage appears to stimulate DNRA. Within the Orca Basin brine pool and

its immediate surroundings, our isotopic data confirms that the composition of sinking biomass preserves the composition of seawater nitrate, as previously proposed (Meckler et al., 2011). We also find tentative evidence of microbial ammonium recycling within the brine pool, but further analyses are required to confirm this proposition. In conclusion, our data add to growing evidence that brine seeps stimulate diverse microbial nitrogen metabolisms, which impact the sedimentary isotopic archive and may be preserved in ancient strata.

## Data Availability Statement

All data generated in this project are presented in Tables S1–S2 in the supplements, and they are available from the National Geoscience Data Centre of the British Geological Survey under https://doi.org/10.5285/39988664-4361-4bee-a4ad-3f40931890c6.

**Acknowledgments**
This work was financially supported by a NERC Frontiers Grant (NE/V010824/1) and a Leverhulme Trust Grant (RPG-2022-313) to EES. We thank Angus McLuskie for technical assistance. Sampling in the Gulf of Mexico was supported by NSF (Microbial Observatories 0801741). We thank the crew of RV *Atlantis* and HOV *Alvin* for expert performance during cruise AT18-02. Yang Liu and three anonymous reviewers provided constructive feedback that improved the manuscript.

## References

Abdulgawad, F., Bockelmann, E. B., Sapsford, D., Williams, K. P., & Falconer, R. (2009). Ammonium ion adsorption on clays and sand under freshwater and seawater conditions. In *Advances in water resources and hydraulic engineering* (pp. 656–661).

Altabet, M. A., & Francois, R. (1994). Sedimentary nitrogen isotopic ratio as a recorder for surface ocean nitrate utilization. *Global Biogeochemical Cycles*, *8*(1), 103–116. https://doi.org/10.1029/93gb03396

Anbar, A. D., & Knoll, A. H. (2002). Proterozoic ocean chemistry and evolution: A bioinorganic bridge? *Science*, *297*(5584), 1137–1142. https://doi.org/10.1126/science.1069651

Boetius, A., Elvert, M., Samarkin, V., & Joye, S. B. (2005). Molecular biogeochemistry of sulfate reduction, methanogenesis and the anaerobic oxidation of methane at Gulf of Mexico cold seeps. *Geochimica et Cosmochimica Acta*, *69*(17), 4267–4281. https://doi.org/10.1016/j.gca.2005.04.012

Brandes, J. A., & Devol, A. H. (2002). A global marine-fixed nitrogen isotopic budget: Implications for Holocene nitrogen cycling. *Global Biogeochemical Cycles*, *16*(4). https://doi.org/10.1029/2001GB001856

Brunner, B., Contreras, S., Lehmann, M. F., Matantseva, O., Rollog, M., Kalvelage, T., et al. (2013). Nitrogen isotope effects induced by anammox bacteria. *Proceedings of the National Academy of Sciences of the United States of America*, *110*(47), 18994–18999. https://doi.org/10.1073/pnas.1310488110

Carpenter, E. J., Harvey, H. R., Fry, B., & Capone, D. G. (1997). Biogeochemical tracers of the marine cyanobacterium Trichodesmium. *Deep Sea Research Part I: Oceanographic Research Papers*, *44*(1), 27–38. https://doi.org/10.1016/s0967-0637(96)00091-x

Casciotti, K. L. (2009). Inverse kinetic isotope fractionation during bacterial nitrite oxidation. *Geochimica et Cosmochimica Acta*, *73*(7), 2061–2076. https://doi.org/10.1016/j.gca.2008.12.022

Casciotti, K. L., Sigman, D. M., & Ward, B. B. (2003). Linking diversity and stable isotope fractionation in ammonia-oxidizing bacteria. *Geomicrobiology Journal*, *20*(4), 335–353. https://doi.org/10.1080/01490450303895

Cleaves, H. J., Chalmers, J. H., Lazcano, A., Miller, S. L., & Bada, J. L. (2008). A reassessment of prebiotic organic synthesis in neutral planetry atmospheres. *Origins of Life and Evolution of Biospheres*, *38*(2), 105–115. https://doi.org/10.1007/s11084-007-9120-3

Cowen, J. P., Wen, X., Jones, R. D., & Thomson, R. E. (1998). Elevated $NH_4^+$ in a neutrally buoyant hydrothermal plume. *Deep Sea Research Part I: Oceanographic Research Papers*, *45*(11), 1891–1902. https://doi.org/10.1016/s0967-0637(98)00032-6

Dennen, K. O., Johnson, C. A., Otter, M. L., Silva, S. R., & Wandless, G. A. (2006). $\delta^{15}N$ and non-carbonate $\delta^{13}C$ values for two petroleum source rock reference materials and a marine sediment reference material. U.S. Geological Survey Open-File Report 2006-1071.

Emsbo, P. (2009). Geologic criteria for the assessment of sedimentary exhalative (sedex) Zn-Pb-Ag deposits. US Geological Survey open-file report, 1209, pp. 1–21.

Engelen, B., Nguyen, T., Heyerhoff, B., Kalenborn, S., Sydow, K., Tabai, H., et al. (2021). Microbial communities of hydrothermal Guaymas Basin surficial sediment profiled at 2 millimeter-scale resolution. *Frontiers in Microbiology*, *12*. https://doi.org/10.3389/fmicb.2021.710881

Gaines, R. R. (2014). Burgess Shale-type preservation and its distribution in space and time. *Paleontological Society Papers*, *20*, 123–146. https://doi.org/10.1017/s1089332600002837

Gaines, R. R., Hammarlund, E. U., Hou, X., Qi, C., Gabbott, S. E., Zhao, Y., et al. (2012). Mechanism for burgess shale-type preservation. *Proceedings of the National Academy of Sciences of the United States of America*, *109*(14), 5180–5184. https://doi.org/10.1073/pnas.1111784109

Gonzalez, C. A., & Choquette, S. J. (2023). *Reference material 8547, IAEA-N-1 (nitrogen isotopes in ammonium sulfate), reference material information sheet* (pp. 1–5). National Institute of Standards and Technology (NIST), US Department of Commerce.

Grey, J. (2016). The incredible lightness of being methane-fuelled: Stable isotopes reveal alternative energy pathways in aquatic ecosystems and beyond. *Frontiers in Ecology and Evolution*, *4*. https://doi.org/10.3389/fevo.2016.00008

Gruber, N., & Galloway, J. N. (2008). An Earth-system perspective of the global nitrogen cycle. *Nature*, *451*(7176), 293–296. https://doi.org/10.1038/nature06592

Gruber, N., & Sarmiento, J. L. (1997). Global patterns of marine nitrogen fixation and denitrification. *Global Biogeochemical Cycles*, *11*(2), 235–266. https://doi.org/10.1029/97gb00077

Hanz, U., Riekenberg, P., de Kluijver, A., van der Meer, M., Middelburg, J. J., de Goeij, J. M., et al. (2022). The important role of sponges in carbon and nitrogen cycling in a deep-sea biological hotspot. *Functional Ecology*, *36*(9), 2188–2199. https://doi.org/10.1111/1365-2435.14117

Hoch, M. P., Fogel, M. L., & Kirchman, D. L. (1992). Isotope fractionation associated with ammonium uptake by a marine bacterium. *Limnology & Oceanography*, *37*(7), 1447–1459. https://doi.org/10.4319/lo.1992.37.7.1447

Ireland, T., Large, R. R., McGoldrick, P., & Blake, M. (2004). Spatial distribution patterns of sulfur isotopes, nodular carbonate, and ore textures in the McArthur River (HYC) Zn-Pb-Ag deposit, Northern Territory, Australia. *Economic Geology*, *99*(8), 1687–1709. https://doi.org/10.2113/gsecongeo.99.8.1687

Johnston, P. A., Johnston, K. J., Collom, C. J., Powell, W. G., & Pollock, R. J. (2009). Palaeontology and depositional environments of ancient brine seeps in the Middle Cambrian Burgess Shale at The Monarch, British Columbia, Canada. *Palaeogeography, Palaeoclimatology, Palaeoecology*, *277*(1–2), 86–105. https://doi.org/10.1016/j.palaeo.2009.02.013

Joye, S. B., Bowles, M. W., Samarkin, V. A., Hunter, K. S., & Niemann, H. (2010). Biogeochemical signatures and microbial activity of different cold-seep habitats along the Gulf of Mexico deep slope. *Deep Sea Research Part II: Topical Studies in Oceanography*, *57*(21–23), 1990–2001. https://doi.org/10.1016/j.dsr2.2010.06.001

Joye, S. B., MacDonald, I. R., Montoya, J. P., & Peccini, M. (2005). Geophysical and geochemical signatures of Gulf of Mexico seafloor brines. *Biogeosciences*, *2*(3), 295–309. https://doi.org/10.5194/bg-2-295-2005

Knapp, A. N. (2012). The sensitivity of marine N2 fixation to dissolved inorganic nitrogen. *Frontiers in Microbiology*, *3*. https://doi.org/10.3389/fmicb.2012.00374

Knapp, A. N., Sigman, D. M., & Lipschultz, F. (2005). N isotopic composition of dissolved organic nitrogen and nitrate at the Bermuda Atlantic Time-series Study site. *Global Biogeochemical Cycles*, *19*(1). https://doi.org/10.1029/2004GB002320

Koehler, M. C., Stüeken, E. E., Kipp, M. A., Buick, R., & Knoll, A. H. (2017). Spatial and temporal trends in Precambrian nitrogen cycling: A Mesoproterozoic offshore nitrate minimum. *Geochimica et Cosmochimica Acta*, *198*, 315–337. https://doi.org/10.1016/j.gca.2016.10.050

Large, R. R., Bull, S. W., Cooke, D. R., & McGoldrick, P. J. (1998). A genetic model for the HYC Deposit, Australia; based on regional sedimentology, geochemistry, and sulfide-sediment relationships. *Economic Geology*, *93*(8), 1345–1368. https://doi.org/10.2113/gsecongeo.93.8.1345

Large, R. R., Bull, S. W., McGoldrick, P. J., & Walters, S. G. (2005). Stratiform and strata-bound Zn-Pb-Ag deposits in Proterozoic sedimentary basins, northern Australia. *Economic Geology*, *100*, 931–963.

Li, Y., Li, L., & Wu, Z. (2021). First-principles calculations of equilibrium nitrogen isotope fractionations among aqueous ammonium, silicate minerals and salts. *Geochimica et Cosmochimica Acta*, *297*, 220–232. https://doi.org/10.1016/j.gca.2021.01.019

Lloyd, K. G., Albert, D. B., Biddle, J. F., Chanton, J. P., Pizarro, O., & Teske, A. (2010). Spatial structure and activity of sedimentary microbial communities underlying a Beggiatoa spp. mat in a Gulf of Mexico hydrocarbon seep. *PLoS One*, *5*(1), e8738. https://doi.org/10.1371/journal.pone.0008738

Lloyd, K. G., Lapham, L., & Teske, A. (2006). An anaerobic methane-oxidizing community of ANME-1 archaea in hypersaline Gulf of Mexico sediments. *Applied and Environmental Microbiology*, *72*(11), 7218–7230. https://doi.org/10.1128/aem.00886-06

Lyons, T. W., Gellatly, A. M., McGoldrick, P. J., & Kah, L. C. (2006). Proterozoic sedimentary exhalative (SEDEX) deposits and links to evolving global ocean chemistry. In S. E. Kesler & H. Ohmoto (Eds.), *Evolution of early Earth's atmosphere, hydrosphere, and biosphere - constraints from ore deposits*. Geological Society of America Memoir.

Macko, S. A., Fogel, M. L., Hare, P. E., & Hoering, T. C. (1987). Isotopic fractionation of nitrogen and carbon in the synthesis of amino acids by microorganisms. *Chemical Geology*, *65*(1), 79–92. https://doi.org/10.1016/0168-9622(87)90064-9

Magnall, J. M., Gleeson, S. A., Hayward, N., & Rocholl, A. (2020). Massive sulfide Zn deposits in the Proterozoic did not require euxinia. *Geochemical Perspectives Letters*, *13*, 19–24. https://doi.org/10.7185/geochemlet.2008

Mapelli, F., Barozzi, A., Michoud, G., Merlino, G., Crotti, E., Borin, S., & Daffonchio, D. (2017). An updated view of the microbial diversity in deep hypersaline anoxic basins. In H. Stan-Lotter & S. Fendrihan (Eds.), *Adaption of microbial life to environmental extremes: Novel research results and application* (pp. 23–40). Springer Link.

Marconi, D., Weigand, M. A., & Sigman, D. M. (2019). Nitrate isotopic gradients in the North Atlantic Ocean and the nitrogen isotopic composition of sinking organic matter. *Deep Sea Research Part I: Oceanographic Research Papers*, *145*, 109–124. https://doi.org/10.1016/j.dsr.2019.01.010

McCready, R. G. L., Gould, W. D., & Barendregt, R. W. (1983). Nitrogen isotope fractionation during the reduction of NO3-to NH4+ by Desulfovibrio sp. *Canadian Journal of Microbiology*, *29*(2), 231–234. https://doi.org/10.1139/m83-038

Meckler, A. N., Ren, H., Sigman, D. M., Gruber, N., Plessen, B., Schubert, C. J., & Haug, G. H. (2011). Deglacial nitrogen isotope changes in the Gulf of Mexico: Evidence from bulk sedimentary and foraminifera-bound nitrogen in Orca Basin sediments. *Paleoceanography*, *26*(4). https://doi.org/10.1029/2011PA002156

Merlino, G., Barozzi, A., Michoud, G., Ngugi, D. K., & Daffonchio, D. (2018). Microbial ecology of deep-sea hypersaline anoxic basins. *FEMS Microbiology Ecology*, *94*(7). https://doi.org/10.1093/femsec/fiy1085

Minagawa, M., & Wada, E. (1986). Nitrogen isotope ratios of red tide organisms in the East China Sea: A characterization of biological nitrogen fixation. *Marine Chemistry*, *19*(3), 245–259. https://doi.org/10.1016/0304-4203(86)90026-5

Müller, P. J. (1977). CN ratios in Pacific deep-sea sediments: Effect of inorganic ammonium and organic nitrogen compounds sorbed by clays. *Geochimica et Cosmochimica Acta*, *41*(6), 765–776. https://doi.org/10.1016/0016-7037(77)90047-3

Nigro, L. M., Elling, F. J., Hinrichs, K. U., Joye, S. B., & Teske, A. (2020). Microbial ecology and biogeochemistry of hypersaline sediments in Orca Basin. *PLoS One*, *15*(4), e0231676. https://doi.org/10.1371/journal.pone.0231676

Pachiadaki, M. G., Yakimov, M. M., LaCono, V., Leadbetter, E., & Edgcomb, V. (2014). Unveiling microbial activities along the halocline of Thetis, a deep-sea hypersaline anoxic basin. *The ISME Journal*, *8*(12), 2478–2489. https://doi.org/10.1038/ismej.2014.100

Parry, L., & Caron, J. B. (2019). Canadia spinosa and the early evolution of the annelid nervous system. *Science Advances*, *5*(9), eaax5858. https://doi.org/10.1126/sciadv.aax5858

Peel, F. J., Travis, C. J., & Hossack, J. R. (1995). Genetic structural provinces and salt tectonics of the Cenozoic offshore U.S. Gulf of Mexico: A preliminary analysis. In M. P. A. Jackson, D. G. Roberts, & S. Snelson (Eds.), *Salt tectonics: A global perspective* (pp. 153–175). AAPG.

Pilcher, R. S., & Blumstein, R. D. (2007). Brine volume and salt dissolution rates in Orca Basin, northeast Gulf of Mexico. *AAPG Bulletin*, *91*(6), 823–833. https://doi.org/10.1306/12180606049

Pindell, J. L., & Kennan, L. (2009). Tectonic evolution of the Gulf of Mexico, Caribbean and northern South America in the mantle reference frame: An update. *Geological Society, London, Special Publications*, *328*, 1–55. https://doi.org/10.1144/sp328.1

Powell, W. G., Johnston, P. A., Collom, C. J., & Johnston, K. J. (2006). Middle Cambrian brine seeps on the Kicking Horse Rim and their relationship to talc and magnesite mineralization and associated dolomitization, British Columbia, Canada. *Economic Geology*, *101*(2), 431–451. https://doi.org/10.2113/gsecongeo.101.2.431

Roberts, H. H., & Carney, R. S. (1997). Evidence of episodic fluid, gas, and sediment venting on the northern Gulf of Mexico continental slope. *Economic Geology*, *92*(7–8), 863–879. https://doi.org/10.2113/gsecongeo.92.7-8.863

Rütting, T., Boeckx, P., Müller, C., & Klemedtsson, L. (2011). Assessment of the importance of dissimilatory nitrate reduction to ammonium for the terrestrial nitrogen cycle. *Biogeosciences*, *8*(7), 1779–1791. https://doi.org/10.5194/bg-8-1779-2011

Rysgaard, S., Thastum, P., Dalsgaard, T., Christensen, P. B., & Sloth, N. P. (1999). Effects of salinity on NH 4+ adsorption capacity, nitrification, and denitrification in Danish estuarine sediments. *Estuaries*, *22*(1), 21–30. https://doi.org/10.2307/1352923

Salman-Carvalho, V., Fadeev, E., Joye, S. B., & Teske, A. (2016). How clonal is clonal? Genome plasticity across multicellular segments of a "Candidatus Marithrix sp." filament from sulfidic, briny seafloor sediments in the Gulf of Mexico. *Frontiers in Microbiology*, *7*. https://doi.org/10.3389/fmicb.2016.01173

Sangster, D. F. (2018). Toward an integrated genetic model for vent-distal SEDEX deposits. *Mineralium Deposita*, *53*(4), 509–527. https://doi.org/10.1007/s00126-017-0755-3

Sassen, R., Roberts, H., Aharon, R., Larkin, J., Chinn, E., & Carney, R. (1993). Chemosynthetic bacterial mats at cold hydrocarbon seeps Gulf of Mexico continental slope. *Organic Geochemistry*, *20*(1), 77–89. https://doi.org/10.1016/0146-6380(93)90083-n

Schimmelmann, A., Qi, H., Coplen, T. B., Brand, W. A., Fong, J., Meier-Augenstein, W., et al. (2016). Organic reference materials for hydrogen, carbon, and nitrogen stable isotope-ratio measurements: Caffeines, n-alkanes, fatty acid methyl esters, glycines, L-valines, polyethylenes, and oils. *Analytical Chemistry*, *88*(8), 4294–4302. https://doi.org/10.1021/acs.analchem.5b04392

Schroeder, P. A., & McLain, A. A. (1998). Illite-smectites and the influence of burial diagenesis on the geochemical cycling of nitrogen. *Clay Minerals*, *33*(4), 539–546. https://doi.org/10.1180/000985598545877

Schutte, C. A., Teske, A., MacGregor, B. J., Salman-Carvalho, V., Lavik, G., Hach, P., & de Beer, D. (2018). Filamentous giant beggiatoaceae from the Guaymas Basin are capable of both denitrification and dissimilatory nitrate reduction to ammonium. *Applied and Environmental Microbiology*, *84*(15). https://doi.org/10.1128/AEM.02860-02817

Shokes, R. F., Trabant, P. K., Presley, B. J., & Reid, D. F. (1977). Anoxic, Hypersaline Basin in the Northern Gulf of Mexico. *Science*, *196*(4297), 1443–1446. https://doi.org/10.1126/science.196.4297.1443

Sigman, D. M., Altabet, M. A., McCorkle, D. C., Francois, R., & Fischer, G. (2000). The d15N of nitrate in the southern ocean: Nitrogen cycling and circulation in the ocean interior. *Journal of Geophysical Research*, *105*(C8), 19599–19614. https://doi.org/10.1029/2000JC000265

Southam, G., & Saunders, J. A. (2005). The geomicrobiology of ore deposits. *Economic Geology*, *100*(6), 1067–1084. https://doi.org/10.2113/100.6.1067

Stevens, E. N., Bailey, J. V., Flood, B. E., Jones, D. W., Gilhooly, I. I. I. W. P., Joye, S. B., et al. (2015). Barite encrustation of benthic sulfide-oxidizing bacteria at a marine cold seep. *Geobiology*, *13*(6), 588–603. https://doi.org/10.1111/gbi.12154

Stüeken, E., Long, A., Rochelle-Bates, N., & Teske, A. (2024). Nitrogen isotope and abundance data from brine seeps in the Gulf of Mexico [Dataset]. https://doi.org/10.5285/39988664-4361-4bee-a4ad-3f40931890c6

Stüeken, E. E., Gregory, D. D., Mukherjee, I., & McGoldrick, P. (2021). Sedimentary exhalative venting of bioavailable nitrogen into the early ocean. *Earth and Planetary Science Letters*, *565*, 116963. https://doi.org/10.1016/j.epsl.2021.116963

Tesdal, J. E., Galbraith, E. D., & Kienast, M. (2013). Nitrogen isotopes in bulk marine sediment: Linking seafloor observations with subseafloor records. *Biogeosciences*, *10*(1), 101–118. https://doi.org/10.5194/bg-10-101-2013

Teske, A. (2010). Cryptic links in the ocean. *Science*, *330*(6009), 1326–1327. https://doi.org/10.1126/science.1198400

Teske, A., & Carvalho, V. (2020). Large sulfur-oxidizing bacteria at Gulf of Mexico hydrocarbon seeps. In A. Teske & V. Carvalho (Eds.), *Marine hydrocarbon seeps: Microbiology and biogeochemistry of a global marine habitat* (pp. 149–171). Springer Link.

Teske, A., & Joye, S. B. (2020). The Gulf of Mexico: An introductory survey of a seep-dominated seafloor landscape. In A. Teske & V. Carvalho (Eds.), *Marine hydrocarbon seeps: Microbiology and biogeochemistry of a global marine habitat* (pp. 69–100). Springer Link.

Tribovillard, N., Bout-Roumazeilles, V., Algeo, T., Lyons, T. W., Sionneau, T., Montero-Serrano, J. C., et al. (2008). Paleodepositional conditions in the Orca Basin as inferred from organic matter and trace metal contents. *Marine Geology*, *254*(1–2), 62–72. https://doi.org/10.1016/j.margeo.2008.04.016

Van Cappellen, P., Viollier, E., Roychoudhury, A., Clark, L., Ingall, E., Lowe, K., & Dichristina, T. (1998). Biogeochemical cycles of manganese and iron at the oxic− anoxic transition of a stratified marine basin (Orca Basin, Gulf of Mexico). *Environmental Science and Technology*, *32*(19), 2931–2939. https://doi.org/10.1021/es980307m

Wankel, S. D., Joye, S. B., Samarkin, V. A., Shah, S. R., Friederich, G., Melas-Kyriazi, J., & Girguis, P. R. (2010). New constraints on methane fluxes and rates of anaerobic methane oxidation in a Gulf of Mexico brine pool via in situ mass spectrometry. *Deep Sea Research Part II: Topical Studies in Oceanography*, *57*(21–23), 2022–2029. https://doi.org/10.1016/j.dsr2.2010.05.009

Waser, N. A. D., Harrison, P. J., Nielsen, B., Calvert, S. E., & Turpin, D. H. (1998). Nitrogen isotope fractionation during the uptake and assimilation of nitrate, nitrite, ammonium, and urea by a marine diatom. *Limnology & Oceanography*, *43*(2), 215–224. https://doi.org/10.4319/lo.1998.43.2.0215

Williams, N. (1978). Studies of the base metal sulfide deposits at McArthur River, Northern Territory, Australia; II, The sulfide-S and organic-C relationships of the concordant deposits and their significance. *Economic Geology*, *73*(6), 1036–1056. https://doi.org/10.2113/gsecongeo.73.6.1036

Williford, K. H., Grice, K., Logan, G. A., Chen, J., & Huston, D. (2011). The molecular and isotopic effects of hydrothermal alteration of organic matter in the Paleoproterozoic McArthur River Pb/Zn/Ag ore deposit. *Earth and Planetary Science Letters*, *301*(1–2), 382–392. https://doi.org/10.1016/j.epsl.2010.11.029

Winkel, M., De Beer, D., Lavik, G., Peplies, J., & Mussmann, M. (2014). Close association of active nitrifyers with Beggiatoa mats covering deep-sea hydrothermal sediments. *Environmental Microbiology*, *16*(6), 1612–1626. https://doi.org/10.1111/1462-2920.12316

Yamanaka, T., Sakamoto, A., Kiyokawa, K., JaeGuk, J., Onishi, Y., Kuwahara, Y., et al. (2024). Nitrogen isotope homogenization of dissolved ammonium through depth and 15N enrichment of ammonium during the incorporation into expandable layer silicates occurred in organic-rich marine sediment from Guaymas Basin, Gulf of California. *Chemical Geology*, 122203. https://doi.org/10.1016/j.chemgeo.2024.122203

Yu, A. J., Lin, X., Zhu, J., He, H., & Li, L. (2023). Environmental effects on ammonium adsorption onto clay minerals: Experimental constraints and applications. *Applied Clay Science*, *246*, 107165. https://doi.org/10.1016/j.clay.2023.107165

Zerkle, A., Junium, C. K., Canfield, D. E., & House, C. H. (2008). Production of $^{15}$N-depleted biomass during cyanobacterial $N_2$-fixation at high Fe concentrations. *Journal of Geophysical Research*, *113*(G3). https://doi.org/10.1029/2007JG000651

Zhang, S., Fang, Y., & Xi, D. (2016). Adaptation of micro-diffusion method for the analysis of 15N natural abundance of ammonium in samples with small volume. *Rapid Communications in Mass Spectrometry*, *29*(14), 1297–1306. https://doi.org/10.1002/rcm.7224

Zhang, X., Sigman, D. M., Morel, F. M., & Kraepiel, A. M. (2014). Nitrogen isotope fractionation by alternative nitrogenases and past ocean anoxia. *Proceedings of the National Academy of Sciences of the United States of America*, *111*(13), 4782–4787. https://doi.org/10.1073/pnas.1402976111